ChemPubSoc Europe

DOI: 10.1002/chem.201704431

CHEMISTRY
A European Journal
Communication

Supramolecular Chemistry

Stoichiometry-Controlled Inversion of Supramolecular Chirality in Nanostructures Co-assembled with Bipyridines

Fang Wang and Chuan-Liang Feng*[a]

Abstract: To control supramolecular chirality of the co-assembled nanostructures, one of the remaining issues is how stoichiometry of the different molecules involved in co-assembly influence chiral transformation. Through co-assembly of achiral 1,4-bis(pyrid-4-yl)benzene and chiral phenylalanine-glycine derivative hydrogelators, stoichiometry is found to be an effective tool for controlling supramolecular chirality inversion processes. This inversion is mainly mediated by a delicate balance between intermolecular hydrogen bonding interactions and π–π stacking of the two components, which may subtly change the stacking of the molecules, in turn, the self-assembled nanostructures. This study exemplifies a simplistic way to invert the handedness of chiral nanostructures and provide fundamental understanding of the inherent principles of supramolecular chirality.

Supramolecular chirality is of vital importance in the fields of biological processes,[1] medicine,[2] asymmetric catalysis,[3] chiral recognition and separation.[4] The creation of artificial chiral structures in relation to molecular design and self-assembly from either amphiphiles,[5] C2/C3-symmetric molecules,[6] π-conjugated molecules,[7] or multiple molecular components[8] are extensively investigated. For example, the controlled supramolecular chirality in chiral systems has been documented upon co-assembly with achiral molecules,[9] which is very useful for understanding the origin of chirality in supramolecular systems or in biological research.[10] Nevertheless, there is still a key question to be answered, that is, the influence of stoichiometric ratio of achiral molecules on supramolecular chirality and the related interaction mechanism, which is a critical issue to clarify the relationship between supramolecular and molecular chirality in biological systems.[11]

Supramolecular chirality describes the chirality of the supramolecular regimes based on non-covalent interactions such as hydrogen bonding, van der Waals interactions, hydrophobic interactions, π–π stacking and so on.[12] These interactions provide an opportunity to regulate the supramolecular chirality in self-assembled systems. Chirality inversion driven by external stimuli has already been reported.[6a,13] Typically, the controllable chirality of supramolecular structures triggered by achiral molecules opens up great possibilities for the design and fabrication of functional chiral materials.[9] However, non-covalent interactions in two-component systems are usually influenced by stoichiometric ratio because of stereoeffect and available bonding positions, which has great influence on the properties of composite hydrogels, such as morphologies, mechanical properties and chirality.[14] Among them, there are scarcely any reports on how stoichiometry influences chiral transformation of co-assembled hydrogels, for example, the chirality control of zinc bisporphyrin systems.[15] However, the control is mainly regulated by coordination interactions, which can only be applied for specific systems. Therefore, the control of supermolecular chirality by stoichiometry under common non-covalent interactions (e.g., hydrogen bonds) is still a challenge.

Here, the co-assembled systems composed of C2-symmetric phenylalanine-glycine-based enantiomers (left-handed LPPG and right-handed DPPG) and bipyridines (DPa, DPe and DPb; Scheme 1, take LPPG as an example) are developed. PPG (LPPG or DPPG enantiomers) with DPa or DPe cannot form chiral nanostructures. A phenomenon of chirality inversion induced by stoichiometry in PPG/DPb system is observed, which is also synchronized with the molecular chiral-interaction inversion. It

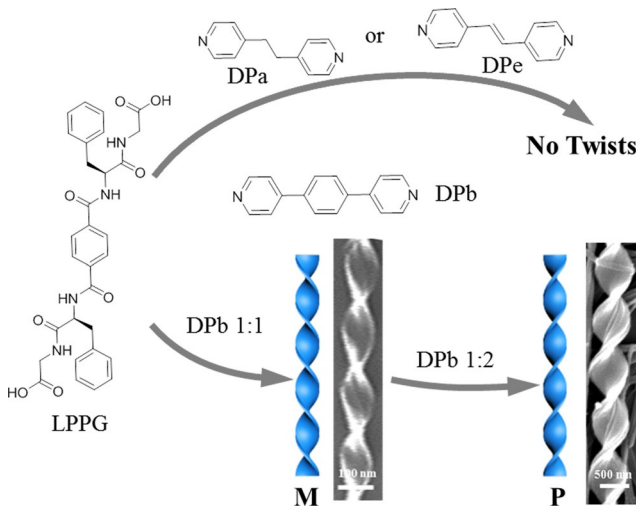

Scheme 1. Molecular structures of LPPG and bipyridines (DPx), and schematic illustration of nanostructures co-assembled from LPPG with achiral bipyridines (DPa, DPe and DPb) at different ratios. M and P denote left- and right-handed chiral nanostructures, respectively.

[a] F. Wang, Prof. C.-L. Feng
State Key Laboratory of Metal Matrix Composites
School of Materials Science and Engineering
Shanghai Jiao Tong University, Shanghai 200240 (P. R. China)
E-mail: clfeng@sjtu.edu.cn

Supporting information and the ORCID identification number for the author of this article can be found under: https://doi.org/10.1002/chem.201704431.

is found that the intermolecular hydrogen bonds and π–π stacking between the enantiomers and the achiral molecules are crucial factors for the inversion. For PPG/DPb = 1:1, strong carboxylic acid-pyridine hydrogen bonds are formed, which drive the building blocks to co-assemble in a head-to-tail fashion. Whereas for PPG/DPb = 1:2, one pyridyl of DPb form an H-bond with PPG, and the other is free in PPG/DPb complex, leading to the formation of 1D aggregates with strong exciton coupling owing to the large conjugated structure of DPb. These two kinds of packing models further induce different chiral rearrangements for the assemblies. The study may develop a methodology to simulate chirality related interactions in biological or self-assembled aggregates just by optimizing the stoichiometry of the assembled complexes.[16]

LPPG and DPPG were synthesized through a conventional liquid-phase reaction according to our previous work (Supporting Information, Figures S1–S6).[17] DPa, DPe and DPb are commercially available. The self-assemblies of PPG with bipyridines were performed in aqueous solution by a heating and cooling process. A racemic mixture of PPG was not used in this study. Both LPPG and DPPG self-assembled into white nanofibrous hydrogels (Figures S7 and S8). Bis(pyridinyl) derivative (DPa, DPe or DPb) was then mixed with PPG in different molar ratios (Figure S7). Solutions were formed for PPG/DPa. Transparent hydrogels and solutions were formed for PPG/DPe = 1:1 and 1:2, respectively. In contrast, white hydrogels were presented for PPG/DPb, but some of DPb precipitated out when the ratio was above 1:2. The minimum gelation concentrations (based on a tube inversion method) of PPG, PPG/DPe = 1:1 and PPG/DPb = 1:1 (or 1:2) were 0.2, 0.1, and 0.05 % w/v, respectively. All of the hydrogels were stable at room temperature for months. Rheological studies further revealed hydrogel formation of PPG with DPe or DPb (Figure S9). The storage modulus (*G*′) was larger than the loss modulus (*G*″), suggesting an elastic rather than viscous material and a rheological feature associated with gel materials.[18] Compared with PPG hydrogel, the detected values of *G*′ and *G*″ were approximately an order of magnitude larger, indicating a better mechanical stability for the co-assembled hydrogels.

The self-assembled nanostructures from PPG/DPx hydrogels were studied by scanning electron microscopy (SEM) measurements (Figures 1 and S10–S13 in the Supporting Information). To systematically investigate the nature of the assembly of PPG/DPb, we varied the mixing ratio continuously. At LPPG/DPb = 1:0.5, the nanofibers started to twist left (Figure S10a). On further increasing the amount of DPb, uniform left-handed (*M*) twisted ribbons with a pitch of about 0.41 μm and a width of about 90 nm were observed for LPPG/DPb = 1:1 (Figures 1 a and S10b). However, continuous increase in molar ratio (LPPG/DPb = 1:1.5) derived the simultaneous formation of both left- and right-handed twists (Figure S10c). Unexpected right-handed (P) twisted ribbons or big twists with pitches of 0.77–4.51 μm and widths of 90–730 nm were achieved for LPPG/DPb = 1:2 (Figures 1 b and S10d). By contrast, the nanofibers started to twist right for DPPG/DPb = 1:0.5 (Figure S10e) and right-handed twisted ribbons with a pitch of about 0.24 μm and a width of about 70 nm were formed for DPPG/DPb = 1:1

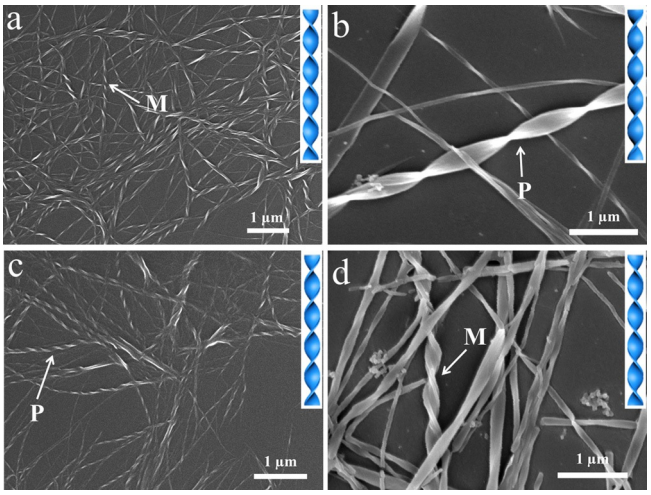

Figure 1. SEM images of: a) left-handed twisted ribbons in the LPPG/DPb = 1:1 xerogel, b) right-handed twisted ribbons in the LPPG/DPb = 1:2 xerogel, c) right-handed twisted ribbons in the DPPG/DPb = 1:1 xerogel, and d) left-handed twisted ribbons in the DPPG/DPb = 1:2 xerogel.

(Figures 1 c and S10f). Increasing the molar ratio of DPPG/DPb to 1:1.5, both left- and right-handed twists were also obtained (Figure S10g). Left-handed twisted nanoribbons for DPPG/DPb = 1:2 were identified that were 0.52–2.46 μm in chiral pitches and 80–620 nm in widths (Figures 1 d and S10h). We also found that thick fibrillar bundles and flat ribbons were formed by the intertwining of a few long slender twists, suggesting that the gelator molecules tend to self-assemble along the 1D fibrillar direction (Figures 1 c and S11). These results indicated that nanoscale twists of opposite handedness could be generated with the variation of stoichiometric ratio of the two components. PPG/DPa exhibited irregular nanostructures at both investigated stoichiometries (Figure S12). A possible interpretation for this may lie in the flexibility of DPa, which lacks the required rigidity to support the 3D framework of the self-assembled supramolecular structures. Non-chiral nanofibers of several micrometers in length were formed for PPG/DPe = 1:1 (Figure S13a, c), whereas irregular nanostructures and nanofibers were both formed for PPG/DPe = 1:2 (Figure S13b, d). All these results strongly suggested that the PPG molecules could interact with all three DPx molecules, giving rise to distinct co-assembly behaviors according to the structural differences of DPx and the stoichiometric ratio of the two components.

Circular dichroism (CD) spectra were employed to further characterize the nanoscale chirality. For LPPG hydrogels, a positive Cotton effect was observed at 276 nm, which was assigned to the intramolecular transitions from the amide linkage to the central aryl group,[9a] whereas the DPPG hydrogels exhibited a negative Cotton effect at 279 nm (Figure S14 in the Supporting Information). For LPPG/DPb hydrogels, significant CD signals were obtained (Figure 2 a). At LPPG/DPb = 1:1, the positive Cotton effect of LPPG at 273 nm and two new cotton effects (−/+) at 316 and 366 nm appeared, which corresponded to the electronic transition of the DPb rings (Figure S15c). However, a negative Cotton effect of LPPG at 258 nm and two new cotton effects (+/−) at 289 and 327 nm of DPb were

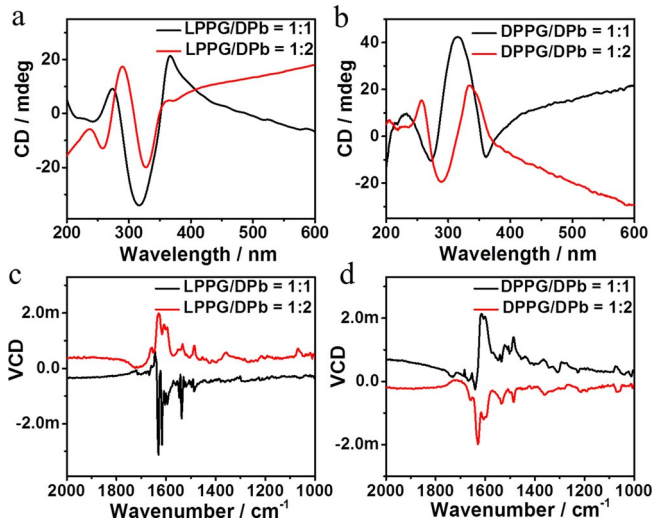

Figure 2. CD and VCD spectra of LPPG/DPb (a, c) and DPPG/DPb (b, d) at molar ratios of 1:1 and 1:2 with the total gelators concentration of 0.1 wt%.

found for LPPG/DPb = 1:2. In the case of DPPG/DPb, the mirror images of the CD spectrums were obtained (Figure 2b), indicating a distinct π–π stacking mode for PPG/DPb = 1:1 compared to that for PPG/DPb = 1:2. With increasing ratio of PPG to DPb from 1:0.5 to 1:1, the CD signal gradually became stronger without shift (Figure S15a), ascribing to the gradual co-assembly of the mixtures. The CD spectral profiles were also inverted and gradually increased in intensity accompanied by blue-shift when adjusting the ratio of PPG/DPb from 1:1.5 to 1:2 (Figure S15b). The results were in good agreement with the SEM results. Moreover, the maximum absorption peak at 305 nm in the UV/Vis spectra for PPG/DPb = 1:1 because of the π–π transition of DPb was blue-shifted to 287 nm for PPG/DPb = 1:2 correspondingly, meaning that the π–π stacking interactions weaken (Figure S15c). For PPG/DPe (Figure S16a in the Supporting Information), a new Cotton effect emerged compared to PPG and the intensity increased with red-shift when the ratio was changed from 1:0.5 to 1:1. Moreover, the CD signals gradually decreased in intensity accompanied by red-shift without inversion by increasing ratio of PPG/DPe from 1:1.5 to 1:2. PPG/DPa also showed CD signals different from PPG (Figure S16b). However, PPG/DPe and PPG/DPa did not exhibit obvious chiral nanostructures. These indicate that DPb induced more effective expression of chirality in the assemblies than DPe and DPa. Furthermore, the reversed supramolecular chirality of PPG/DPb at different ratios results from the formation of distinct aggregates of opposite handedness, and the presence of larger conjugated structure and more planar backbones in DPb induce a more-efficient π–π stacking that stabilize the chiral aggregates than that of DPa and DPe, which lead to the chirality transfer and inversion.

To investigate the gel behaviors and the assembly mechanism of these nanostructures, ^{1}H NMR in D_2O were measured (Figures S17–S20 in the Supporting Information). For PPG/DPb system, because of the strong electron absorbing effect of the carboxyl groups in the PPG structure, the signals of the heteroaromatic protons in DPb were steadily shifted downfield (e.g., proton **a** of the pyridine ring is shifted from 8.50 to 8.61 ppm, and proton **b** of the pyridine ring is shifted from 7.69 to 7.95 ppm; Figure S18). This suggested that hydrogen bonds were formed between the pyridinyl moiety and carboxyl group in the co-assembled hydrogel system. The broadening and decrease in the intensity of the NMR resonance signals can be interpreted as an indication of a restricted freedom of motion.[19] The signal resonance of proton **c** from phenyl rings of DPb disappeared, maybe because it was also shifted downfield and overlapped with proton **b**. To support this, the temperature-dependent ^{1}H NMR spectra of PPG/DPb = 1:1 hydrogel are shown in Figure S17. The signals were strongly broadened in the gel state and gradually became sharper and stronger with increasing temperature, owing to the dissociation of self-assembled aggregates. Especially, a new signal appeared at about 7.84 ppm which should be ascribed to the signal resonance from phenyl rings of DPb, indicating the aromatic π–π stacking. The observation demonstrated that the molecular aggregation of PPG/DPb at room temperature is mainly due to the carboxylic acid-pyridine hydrogen bonds and π–π stacking between the molecules. ^{1}H NMR spectra of PPG/DPe and PPG/DPa at ratios of 1:1 and 1:2 showed similar shifting patterns even though there were more signals at room temperature, due to the existence of different nanostructures (Figures S19 and S20). This suggested that acid-pyridyl hydrogen bonds were also formed in PPG/DPe and PPG/DPa gels.

FTIR and VCD measurements provide valuable information about the molecular-level interaction and chirality of the supramolecular aggregates.[20] The xerogel of PPG was first characterized by FTIR and showed well-defined amide I bands at 1632 cm^{-1}, amide II bands at 1533 cm^{-1}, N–H stretching vibrations at 3445 and 3289 cm^{-1}, and stretching vibration bands of C=O from carboxyl groups at 1736 cm^{-1} (Figure S21 in the Supporting Information), indicating that the amide groups formed strong hydrogen bonds. However, the vibration at 1736 and 3289 cm^{-1} disappeared for PPG/DPb xerogels at different ratios and new bands at 1630 and 1540 cm^{-1} were simultaneously observed, indicating the carboxylic acid-pyridine hydrogen bonds were formed between PPG and DPb. The FTIR spectra of PPG/DPe and PPG/DPa were similar to those described above for PPG/DPb (Figure S22), the band at 1736 and 3289 cm^{-1} were decreased, suggesting acid-pyridyl hydrogen bonds in PPG/DPe and PPG/DPa gels.

In VCD spectra, LPPG and LPPG/DPe = 1:1 exhibited the same (−/+) pattern of C=O stretching band between 1750 and 1600 cm^{-1} (Figure S23 in the Supporting Information). Moreover, DPPG and DPPG/DPe = 1:1 showed the opposite (+/−) pattern. The amide I VCD band in LPPG/DPb = 1:1 had a (+/−) pattern, whereas that of LPPG/DPb = 1:2 was the opposite, namely it had a (−/+) signal (Figure 2c). On the contrary, DPPG/DPb was found to be a "mirror image". DPPG/DPb = 1:1 exhibited a (−/+) pattern, but the VCD signal of the band switched to a significant (+/−) pattern for DPPG/DPb = 1:2 (Figure 2d). These VCD patterns implied the inversion of the chirality from a ratio of 1:1 to 1:2 for PPG/DPb. All these observations reveal that the supramolecular chirality of the nano-

structures in the same system is not only determined by the chirality of monomer (PPG), but also influenced by the stacking mode of building blocks through intermolecular hydrogen bonds and π–π stacking during the co-assembling process.

Small-angle X-ray diffraction (SAXRD) was performed to unveil the mechanism of packing of the supramolecular organizations in the PPG/DPb xerogels (Figure 3a). The PPG xerogels showed two clear diffraction peaks, which corresponded to layer spacings of 1.90 and 0.95 nm, based on Bragg's equation; the ratio of 1:1/2 was consistent with an obvious lamellar structure with a *d*-spacing of 1.90 nm.[21] Intermolecular hydrogen bonds between the amide moieties and carboxyl group are the main driving force for the self-assembly of PPG.[17] Due to the fact that different molecules and complex interactions have been involved in PPG/DPb systems, the SAXRD results are relatively complicated. Well-defined patterns of PPG/DPb = 1:1 xerogels display *d*-spacings of 2.32 and 1.16 nm (1/2), indicating a lamellar structure with a larger *d*-spacing of 2.32 nm, although there were maybe not only one layered structure with identical layer distance in the sample.[14f] This indicated that a composite bilayer was formed, in which DPb molecules were packed in an orderly manner between PPG molecules through carboxylic acid-pyridine interactions. However, the XRD patterns of the PPG/DPb = 1:2 xerogels showed significant differences from that of the PPG/DPb = 1:1 xerogels. The corresponding *d*-spacings were 2.15 and 1.08 nm (1/2), suggesting the formation of a lamellar nanostructure in the twisted ribbons with an interlayer distance of 2.15 nm. The shoulder peak of *d* = 2.32 nm further testified that two different packing modes exist. For PPG/DPb system, it was clear that multifarious noncovalent interactions were involved, including carboxylic acid–pyridyl hydrogen bonds, amide–amide hydrogen bonds, and aromatic π–π stacking. The formation of chiral twists may be attributed to synergistic effects among these noncovalent interactions. Figure 3b (take LPPG as an example) shows the possible interactions and the molecular packing of the gelator molecules in different ratios. For PPG/DPb = 1:1, at the early stages of gelation, strong hydrogen bonds are formed between pyridyl nitrogen and the hydroxy group of a carboxylic acid, which drives the building blocks to co-assemble in a head-to-tail fashion, then three dimensional fiber networks are obtained through the formation of hydrogen bonds between amide groups and π–π interactions among DPb. However, for PPG/DPb = 1:2, one pyridyl nitrogen of DPb forms an H-bond with PPG, whereas the other is free in the PPG/DPb = 1:2 complex. The large conjugated structure of DPb is attributed to strong π–π stacking, causing the formation of one-dimensional chiral aggregates, then three dimensional fiber networks are obtained through the formation of hydrogen bonds between amide groups. The overlapping DPb chromophore leading to the *d*-spacing is slightly diminished. These two different molecular packing modes lead to the chirality inversion. Meanwhile, the relative proportions of the two kinds of aggregates could be adjusted by modification of the PPG/DPb ratio.

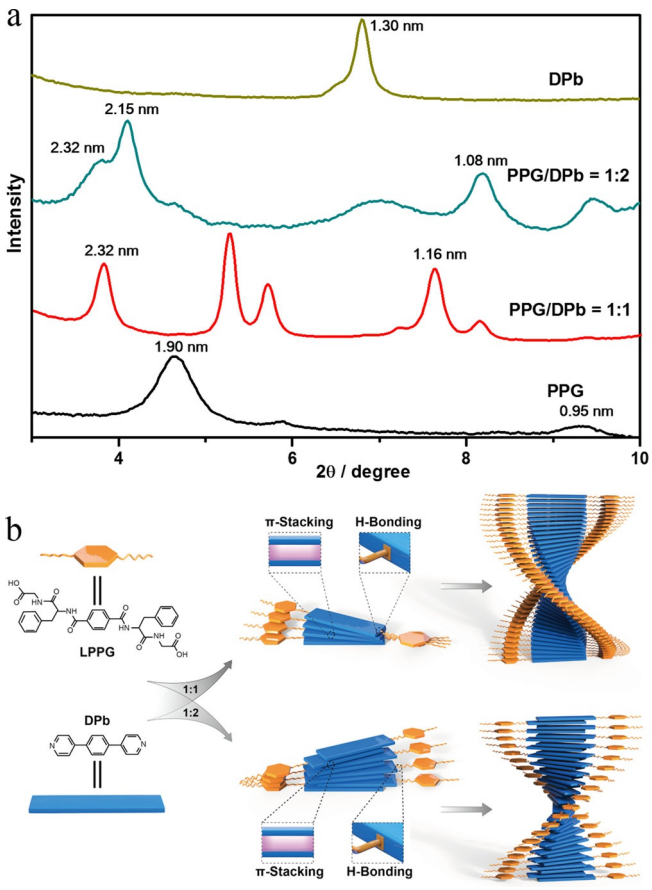

Figure 3. a) SAXRD patterns of the xerogels of PPG, PPG/DPb = 1:1, PPG/DPb = 1:2, and powder DPb; b) schematic illustration of the aggregation pathways of LPPG/DPb at ratios of 1:1 and 1:2.

The inversion of supramolecular chirality can be triggered by stoichiometry in co-assembled nanostructures owning to a delicate balance between hydrogen bonding interactions and π–π stacking of chiral and achiral molecules. This system is a remarkable and rarely observed example of nanostructure handedness based on the co-assembly of a short dipeptide derivative and an achiral molecule that can be easily controlled by stoichiometry. This study is believed to add a new dimension in the field of regulating supramolecular chirality, and provides a better understanding of how achiral molecular can participate in the chiral self-assembly to express unique biological functions.

Experimental Section

Hydrogel preparation

The LPPG/DPb = 1:1 hydrogel with 0.2 wt% LPPG/DPb is used as an example to describe the preparation procedure. LPPG/DPb (2 mg mL^{-1}, 1:1 mixture of LPPG and DPb) was suspended in a septum-capped 5 mL glass vial. The mixture was gently heated at 80–100 °C for few minutes until a transparent solution was appeared, then spontaneous cooling to room temperature (25 °C) and incubating about 2 h. The formation of hydrogel was confirmed by vial inversion test.

Acknowledgements

This work was supported by the NSFC (51573092), the Innovation Program of Shanghai Municipal Education Commission (2017010700002E00061), and the SJTU-UM Collaborative Research, Program for Professors of Special Appointment (Eastern Scholar) at the Shanghai Institutions of Higher Learning.

Conflict of interest

The authors declare no conflict of interest.

Keywords: chiral twists · chirality · co-assembly · stoichiometry · supramolecular chemistry

[1] a) G.-F. Liu, D. Zhang, C.-L. Feng, *Angew. Chem. Int. Ed.* **2014**, *53*, 7789 – 7793; *Angew. Chem.* **2014**, *126*, 7923 – 7927; b) M. Kato, N. Matsumoto, K. K. Sakai, T. Toyóoka, *J. Pharm. Biomed. Anal.* **2003**, *30*, 1845 – 1850; c) R. P. Cheng, S. H. Gellman, W. F. DeGrado, *Chem. Rev.* **2001**, *101*, 3219 – 3232.

[2] a) P. D. Thornton, R. J. Mart, R. V. Ulijn, *Adv. Mater.* **2007**, *19*, 1252 – 1256; b) J. Li, Y. Kuang, Y. Gao, X. Du, J. Shi, B. Xu, *J. Am. Chem. Soc.* **2013**, *135*, 542 – 545.

[3] a) A. Dondoni, A. Massi, *Angew. Chem. Int. Ed.* **2008**, *47*, 4638 – 4660; *Angew. Chem.* **2008**, *120*, 4716 – 4739; b) S. C. Mohapatra, J. T. Hsu, *Biotechnol. Bioeng.* **1999**, *64*, 213 – 220; c) F. Rodríguez-Llansola, B. Escuder, J. F. Miravet, *J. Am. Chem. Soc.* **2009**, *131*, 11478 – 11484; d) F. Rodríguez-Llansola, B. Escuder, J. F. Miravet, *J. Am. Chem. Soc.* **2009**, *131*, 11478 – 11484.

[4] a) A. Kühnle, T. R. Linderoth, B. Hammer, F. Besenbacher, *Nature* **2002**, *415*, 891 – 893; b) W. Edwards, D. K. Smith, *J. Am. Chem. Soc.* **2014**, *136*, 1116 – 1124; c) H. Cao, X. Zhu, M. Liu, *Angew. Chem. Int. Ed.* **2013**, *52*, 4122 – 4126; *Angew. Chem.* **2013**, *125*, 4216 – 4220; d) J. H. Jung, S.-J. Moon, J. Ahn, J. Jaworski, S. Shinkai, *ACS Nano* **2013**, *7*, 2595 – 2601; e) S. M. So, K. Moozeh, A. J. Lough, J. Chin, *Angew. Chem. Int. Ed.* **2014**, *53*, 829 – 832; *Angew. Chem.* **2014**, *126*, 848 – 851; f) K. Kodama, Y. Kobayashi, K. Saigo, *Chem. Eur. J.* **2007**, *13*, 2144 – 2152; g) L. Zhang, L. Qin, X. Wang, H. Cao, M. Liu, *Adv. Mater.* **2014**, *26*, 6959 – 6964; h) H. Jintoku, M. Takafuji, R. Oda, H. Ihara, *Chem. Commun.* **2012**, *48*, 4881 – 4883.

[5] a) H. Cui, A. G. Cheetham, E. T. Pashuck, S. I. Stupp, *J. Am. Chem. Soc.* **2014**, *136*, 12461 – 12468; b) R. Oda, I. Huc, M. Schmutz, S. J. Candau, F. C. MacKintosh, *Nature* **1999**, *399*, 566 – 569; c) A. Sorrenti, O. Illa, R. M. Ortuño, *Chem. Soc. Rev.* **2013**, *42*, 8200 – 8219; d) M. S. Spector, A. Singh, P. B. Messersmith, J. M. Schnur, *Nano Lett.* **2001**, *1*, 375 – 378; e) M. Liu, L. Zhang, T. Wang, *Chem. Rev.* **2015**, *115*, 7304 – 7397.

[6] a) G. Qing, X. Shan, W. Chen, Z. Lv, P. Xiong, T. Sun, *Angew. Chem. Int. Ed.* **2014**, *53*, 2124 – 2129; *Angew. Chem.* **2014**, *126*, 2156 – 2161; b) F. García, J. Buendía, L. Sánchez, *J. Org. Chem.* **2011**, *76*, 6271 – 6276; c) Y. Nakano, T. Hirose, P. J. M. Stals, E. W. Meijer, A. R. A. Palmans, *Chem. Sci.* **2012**, *3*, 148 – 155; d) F. Wang, M. A. J. Gillissen, P. J. M. Stals, A. R. A. Palmans, E. W. Meijer, *Chem. Eur. J.* **2012**, *18*, 11761 – 11770; e) C. Moberg, *Angew. Chem. Int. Ed.* **1998**, *37*, 248 – 268; *Angew. Chem.* **1998**, *110*, 260 – 281; f) Y. Dai, X. Zhao, X. Su, G. Li, A. Zhang, *Macromol. Rapid Commun.* **2014**, *35*, 1326 – 1331.

[7] a) A. Ajayaghosh, C. Vijayakumar, R. Varghese, S. J. George, *Angew. Chem. Int. Ed.* **2006**, *45*, 456 – 460; *Angew. Chem.* **2006**, *118*, 470 – 474; b) S. Bai, S. Debnath, N. Javid, P. W. J. M. Frederix, S. Fleming, C. Pappas, R. V. Ulijn, *Langmuir* **2014**, *30*, 7576 – 7584; c) S. S. Babu, V. K. Praveen, A. Ajayaghosh, *Chem. Rev.* **2014**, *114*, 1973 – 2129.

[8] a) K. Lv, L. Qin, X. Wang, L. Zhang, M. Liu, *Phys. Chem. Chem. Phys.* **2013**, *15*, 20197 – 20202; b) Y. Tsunoda, K. Fukuta, T. Imamura, R. Sekiya, T. Furuyama, N. Kobayashi, T. Haino, *Angew. Chem. Int. Ed.* **2014**, *53*, 7243 – 7247; *Angew. Chem.* **2014**, *126*, 7371 – 7375; c) K. Watanabe, H. Iida, K. Akagi, *Adv. Mater.* **2012**, *24*, 6451 – 6456; d) W. Zhang, M. Fujiki, X. Zhu, *Chem. Eur. J.* **2011**, *17*, 10628 – 10635; e) S. K. Samanta, S. Bhattacharya, *Chem. Commun.* **2013**, *49*, 1425 – 1427; f) C. F. J. Faul, *Acc. Chem. Res.* **2014**, *47*, 3428 – 3438.

[9] a) G.-F. Liu, L.-Y. Zhu, W. Ji, C.-L. Feng, Z.-X. Wei, *Angew. Chem. Int. Ed.* **2016**, *55*, 2411 – 2415; *Angew. Chem.* **2016**, *128*, 2457 – 2461; b) G. Liu, J. Liu, C. Feng, Y. Zhao, *Chem. Sci.* **2017**, *8*, 1769 – 1775.

[10] a) A. Ajayaghosh, R. Varghese, S. J. George, C. Vijayakumar, *Angew. Chem. Int. Ed.* **2006**, *45*, 1141 – 1144; *Angew. Chem.* **2006**, *118*, 1159 – 1162; b) Y. Li, T. Wang, M. Liu, *Soft Matter* **2007**, *3*, 1312 – 1317; c) Y. Wang, W. Qi, R. Huang, X. Yang, M. Wang, R. Su, Z. He, *J. Am. Chem. Soc.* **2015**, *137*, 7869 – 7880; d) M. Deng, L. Zhang, Y. Jiang, M. Liu, *Angew. Chem. Int. Ed.* **2016**, *55*, 15062 – 15066; *Angew. Chem.* **2016**, *128*, 15286 – 15290; e) T. Seki, A. Asano, S. Seki, Y. Kikkawa, H. Murayama, T. Karatsu, A. Kitamura, S. Yagai, *Chem. Eur. J.* **2011**, *17*, 3598 – 3608.

[11] a) A. R. Hirst, J. F. Miravet, B. Escuder, L. Noirez, V. Castelletto, I. W. Hamley, D. K. Smith, *Chem. Eur. J.* **2009**, *15*, 372 – 379; b) D. J. Selkoe, *Nature* **2003**, *426*, 900 – 904; c) A. R. Hirst, D. K. Smith, M. C. Feiters, H. P. Geurts, *Chem. Eur. J.* **2004**, *10*, 5901 – 5910; d) D. Bandyopadhyay, D. Prashar, Y.-Y. Luk, *Chem. Commun.* **2011**, *47*, 6165 – 6167.

[12] a) T. Tu, W. Fang, X. Bao, X. Li, K. H. Dötz, *Angew. Chem. Int. Ed.* **2011**, *50*, 6601 – 6605; *Angew. Chem.* **2011**, *123*, 6731 – 6735; b) B. Adhikari, J. Nanda, A. Banerjee, *Soft Matter* **2011**, *7*, 8913 – 8922; c) Z. Shen, T. Wang, M. Liu, *Chem. Commun.* **2014**, *50*, 2096 – 2099; d) P. Duan, H. Cao, L. Zhang, M. Liu, *Soft Matter* **2014**, *10*, 5428 – 5448; e) L. Frkanec, M. Žinić, *Chem. Commun.* **2010**, *46*, 522 – 537; f) Y. Rong, P. Chen, D. Wang, M. Liu, *Langmuir* **2012**, *28*, 6356 – 6363.

[13] a) Y. Yan, K. Deng, Z. Yu, Z. Wei, *Angew. Chem. Int. Ed.* **2009**, *48*, 2003 – 2006; *Angew. Chem.* **2009**, *121*, 2037 – 2040; b) Y. Yan, Z. Yu, Y. W. Huang, W. X. Yuan, Z. X. Wei, *Adv. Mater.* **2007**, *19*, 3353 – 3357; c) J. M. Ribó, J. Crusats, F. Sagués, J. Claret, R. Rubires, *Science* **2001**, *292*, 2063 – 2066; d) S. I. Sakurai, K. Okoshi, J. Kumaki, E. Yashima, *J. Am. Chem. Soc.* **2006**, *128*, 5650 – 5651; e) M. Peterca, M. R. Imam, C.-H. Ahn, V. S. K. Balagurusamy, D. A. Wilson, B. M. Rosen, V. Percec, *J. Am. Chem. Soc.* **2011**, *133*, 2311 – 2328; f) A. Gopal, M. Hifsudheen, S. Furumi, M. Takeuchi, A. Ajayaghosh, *Angew. Chem. Int. Ed.* **2012**, *51*, 10505 – 10509; *Angew. Chem.* **2012**, *124*, 10657 – 10661; g) J. Kumar, T. Nakashima, T. Kawai, *Langmuir* **2014**, *30*, 6030 – 6037; h) D. Kurouski, X. Lu, L. Popova, W. Wan, M. Shanmugasundaram, G. Stubbs, R. K. Dukor, I. K. Lednev, L. A. Nafie, *J. Am. Chem. Soc.* **2014**, *136*, 2302 – 2312.

[14] a) A. R. Hirst, D. K. Smith, J. P. Harrington, *Chem. Eur. J.* **2005**, *11*, 6552 – 6559; b) W. Edwards, D. K. Smith, *J. Am. Chem. Soc.* **2013**, *135*, 5911 – 5920; c) S. Bhattacharjee, S. Datta, S. Bhattacharya, *Chem. Eur. J.* **2013**, *19*, 16672 – 16681; d) S. Bhattacharjee, S. Bhattacharya, *Chem. Commun.* **2015**, *51*, 6765 – 6768; e) P. Bairi, B. Roy, A. K. Nandi, *J. Phys. Chem. B* **2010**, *114*, 11454 – 11461; f) Y. Liu, T. Wang, M. Liu, *Chem. Eur. J.* **2012**, *18*, 14650 – 14659; g) X. Zhu, P. Duan, L. Zhang, M. Liu, *Chem. Eur. J.* **2011**, *17*, 3429 – 3437.

[15] a) V. V. Borovkov, J. M. Lintuluoto, Y. Inoue, *Org. Lett.* **2002**, *4*, 169 – 171; b) V. V. Borovkov, J. M. Lintuluoto, G. A. Hembury, M. Sugiura, R. Arakawa, Y. Inoue, *J. Org. Chem.* **2003**, *68*, 7176 – 7192; c) J. Etxebarria, A. Vidal-Ferran, P. Ballester, *Chem. Commun.* **2008**, 5939 – 5941.

[16] S. Zhang, *Nat. Biotechnol.* **2003**, *21*, 1171 – 1178.

[17] F. Wang, W. Ji, J. Liu, J. He, C. Feng, *Macromol. Chem. Phys.* **2017**, *218*, 1600560.

[18] M.-O. M. Piepenbrock, N. Clarke, J. W. Steed, *Langmuir* **2009**, *25*, 8451 – 8456.

[19] M. Tata, V. T. John, Y. Y. Waguespack, G. L. McPherson, *J. Am. Chem. Soc.* **1994**, *116*, 9464 – 9470.

[20] a) M. M. J. Smulders, T. Buffeteau, D. Cavagnat, M. Wolffs, A. P. H. J. Schenning, E. W. Meijer, *Chirality* **2008**, *20*, 1016 – 1022; b) F. Aparicio, B. Nieto-Ortega, F. Nájera, F. J. Ramírez, J. T. L. Navarrete, J. Casado, L. Sánchez, *Angew. Chem. Int. Ed.* **2014**, *53*, 1373 – 1377; *Angew. Chem.* **2014**, *126*, 1397 – 1401.

[21] I. W. Hamley, V. Castelletto, *Prog. Polym. Sci.* **2004**, *29*, 909 – 948.

Manuscript received: September 20, 2017
Accepted manuscript online: December 22, 2017
Version of record online: January 11, 2018